



enhance its properties, namely mechanical and thermal properties, some reinforcement materials are applied as the fillers. Turhan *et al.* [11] attempted to fabricate nanocomposites of PVA/modified bentonite, found that there was an improvement in the thermal stabilities over the pure PVA. The method used was the solution intercalation method. Also, Ferrández-Rives *et al.* [12] conducted the research about PVA/bentonite by using electrospinning, they discovered that the nanocomposites gave better properties for the biomedicine and biotechnology application. In addition, Sang *et al.* [13] prepared composite solid alkaline polymer electrolyte PVA-bentonite-KOH-H<sub>2</sub>O using solution-casting method and found that the interpolation of bentonite to PVA matrix could increase the KOH content in PVA matrix, thus it improved the conductivity of the system particularly at higher water content.

Based on above explanation, this study aims to investigate the characteristics of mechanical properties, morphology and thermal nanoscale composites on the addition of nano mixtures of natural bentonite particles to the PVA polymer using sol-gel method. Sol-gel method is one of the fastest growing chemical fields and is the process of forming inorganic compounds *via* chemical reactions at low temperature solution, while in the process; there is a phase change from the colloidal suspension (sol) to the liquid phase (gel) [14]. It was employed due to its procedure that is based mainly in water soluble polymers, such as PVA. Therefore, the fabrication of nanocomposite PVA/bentonite using sol-gel method should give another perspective of the study about nanocomposites.

## EXPERIMENTAL

The materials used in this study were synthetic bentonite which is obtained from North Tapanuli Pahae District, North Sumatra, Indonesia with size of 35.26 nm [6,15], aquadest and poly(vinyl alcohol) (PVA) pro-analyst purchased from Sigma-Aldrich. The characterization was conducted using several equipments, namely universal testing machine model UCT-5T by Orientec Corporation Ltd. to test mechanical properties, scanning electron microscopy (SEM) EVO MA 10 Zeiss to discover the surface morphology and differential scanning calorimetry (DSC) (Mettler Toledo type 821) to test the thermal properties.

The synthesis of PVA/bentonite nanocomposite was performed by sol gel method. As much as 24 g of PVA were dissolved into 200 mL of distilled water and stirred at 550 rpm and at 80 °C. After the PVA was completely dissolved, bentonite nanoparticles were added into the solution with the variations of 0, 2, 4, 6 and 8 % for 7 h at 80 °C and stirred 550 rpm until thickened to gel. After the solution thickened, it was inserted into the glass mold to dry and harden at room temperature. Then the sample was printed using ISO 527-2 type 1A for Universal Testing Machine UCT-5T model. Then the sample was characterized by using tensile and SEM. DSC was applied to determine the melting point of the nanocomposite PVA/bentonite.

## RESULTS AND DISCUSSION

**Mechanical properties analysis:** The tensile test was performed to evaluate the effect of the addition of bentonite on the mechanical properties of the nanocomposite membrane.

Fig. 1 shows the tensile strength of PVA/bentonite nanocomposites with the variations in the quantity of bentonite. Tensile strength testing on PVA/bentonite showed that there was an enhancement when the clay content increased from 0 to 2 %, but this value dropped when 4 % of bentonite obtained. The fluctuation kept occurring until 8 % of clay content fulfilled. The strength of PVA/bentonite nanocomposites had a maximum value of 6 % by weight of bentonite. The tensile strength of the PVA/bentonite nanocomposites was largely caused by the agglomeration of the organo-clay particles [16]. This result appears to be associated with a lack of interfacial interactions between clays and polymer matrices. Thus, the large number of defects and agglomerations occurred in the interphase region [17-19]. At the strain value, it was found that for each variation indicated a 100 % increasing as shown in Figs. 2 and 3. This increasing occurred because the dispersed nano-bentonite in the polymer matrix will lead to an improvement in the mechanical properties of the membrane nanocomposite. It has been reported that the addition of coated filler particles can easily improve the mechanical properties of the polymer [20].

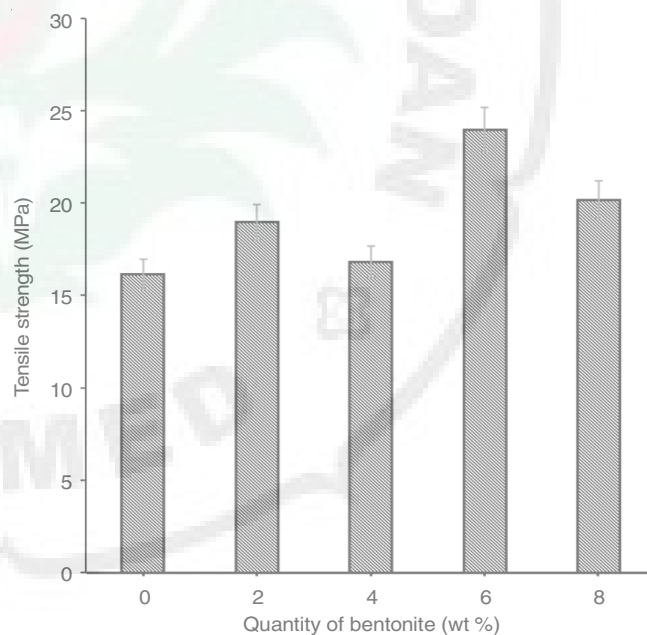


Fig. 1. Tensile strength of PVA/bentonite nanocomposites

Fig. 4 suggests that the addition of bentonite may increase the flexibility of catalyst in PVA [21]. The sharp increase in the addition of nano-bentonite would have an impact on the value of the Young Modulus. It can be assumed that at the high value of increasing in length will cause a low modulus value [22]. Finally, based on Fig. 5, it can be seen from the modulus of elasticity of the 6 % bentonite composition has a higher elasticity modulus value compared to the pure PVA. This increasing occurred because there was a strong interaction between the matrix and silicate layers through the formation of hydrogen bonds due to the strong hydrophilicity of the bentonite edge. However, there was also a decreasing in elasticity modulus value in the variation of 2, 4 and 8 % bentonite. It was due to the deployment of bentonite to the PVA which was uneven [23].

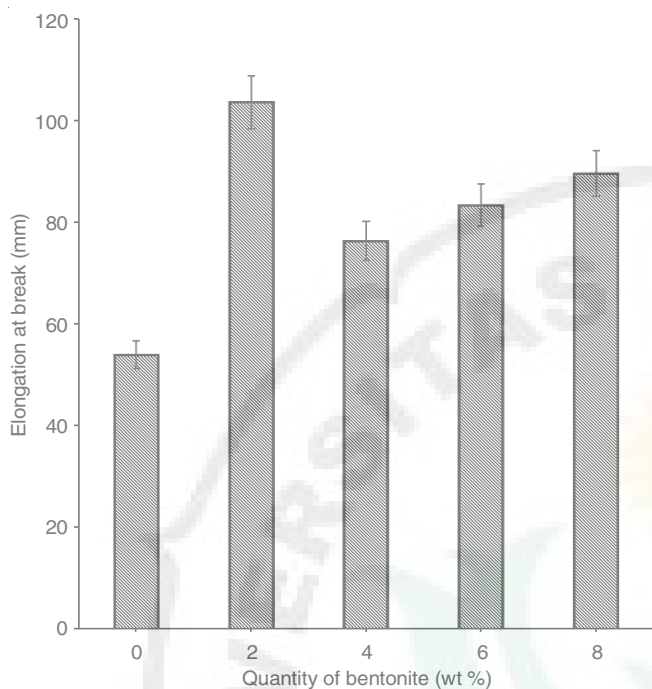


Fig. 2. Elongation at break of PVA/bentonite nanocomposites

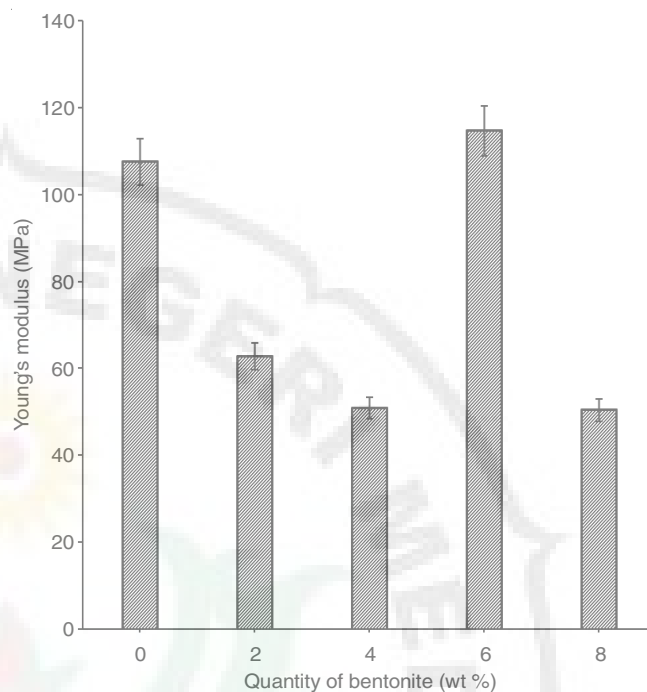


Fig. 4. Young's modulus of PVA/bentonite nanocomposites

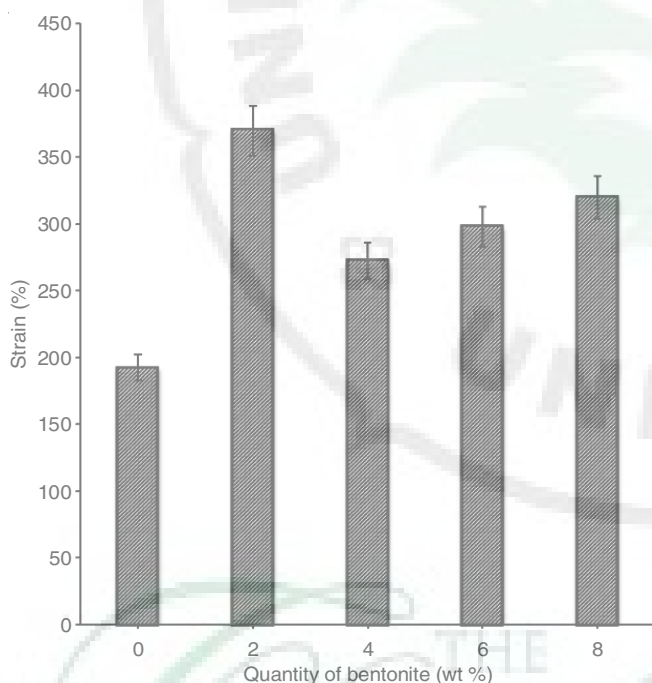


Fig. 3. Strain of PVA/bentonite nanocomposites

**Morphology analysis:** The gel morphology of each variation of the PVA/bentonite nanocomposites in which the nano-bentonite is dispersed on the PVA polymer matrix is shown by Fig. 5. In detail, Fig. 5b, a 2 % PVA/bentonite variation showed a curves and pores on the surface of the gel with a curvature length of 4.122  $\mu\text{m}$ , while the pore length was 1.342  $\mu\text{m}$ . In variation of 4 %, it contained three pores with different sizes, while for variation of 8 % have many pores. For the variation of 6 %, the surface was observed to be flatter, so that fewer pores with a pore length of 0.5237  $\mu\text{m}$  were formed compared to other variations, this was caused by a better bond between the matrix with the filler compared with others.

The connection between PVA with bentonite can be stable because of the hydrogen bond [24]. The interaction rate between the PVA polymer molecule and bentonite particles depends on the polymer concentration in the dispersion [15]. Bentonite can strengthen a crosslinked PVA nanocomposites membrane with various bentonite concentrations [25].

**Thermal properties analysis:** The main information gained from DSC analysis regarding thermal properties is the heat involved in thermal event as a function of time and temperature. The heat involved is commonly expressed in term of enthalpy, which is the amount of heat released or adsorbed by the sample during thermal treatment. The negative value of enthalpy means that the sample adsorbs heat, as indicated by the endothermic peak on the DSC thermogram. In addition, DSC analysis provides quantitative information about melting point and phase transition of the sample [26]. As can be seen in Fig. 6, all samples melt at practically the same temperature, but with different enthalpies. From the analysis of DSC in Fig. 6 and Table-1 on the PVA/bentonite particles (0-8) wt % visible the melting point did not increase significantly with the increase of bentonite at 0 % of melting point value 223.51  $^{\circ}\text{C}$  with enthalpy of 27.10 J/g, however at the 2-6 % composition there is an increase. These results are in accordance with the references (210-230)  $^{\circ}\text{C}$  for full hydrolysis of PVA.

TABLE-1  
RESULTS OF THERMAL TESTING OF  
DSC NANOCOMPOSITE PVA/BENTONITE

Bentonite (wt %)	Temperature ( $^{\circ}\text{C}$ )			Enthalpy ( $\Delta\text{H}$ , J/g)	Heat ( $\Delta\text{Q}$ , mJ)
	Onset	Melting	Endset		
0	209.05	223.51	228.72	27.10	111.12
2	198.41	219.98	224.89	46.83	192.00
4	208.06	222.09	227.24	62.65	256.87
6	208.15	221.95	227.48	49.65	203.56
8	207.27	221.48	227.37	22.71	93.09

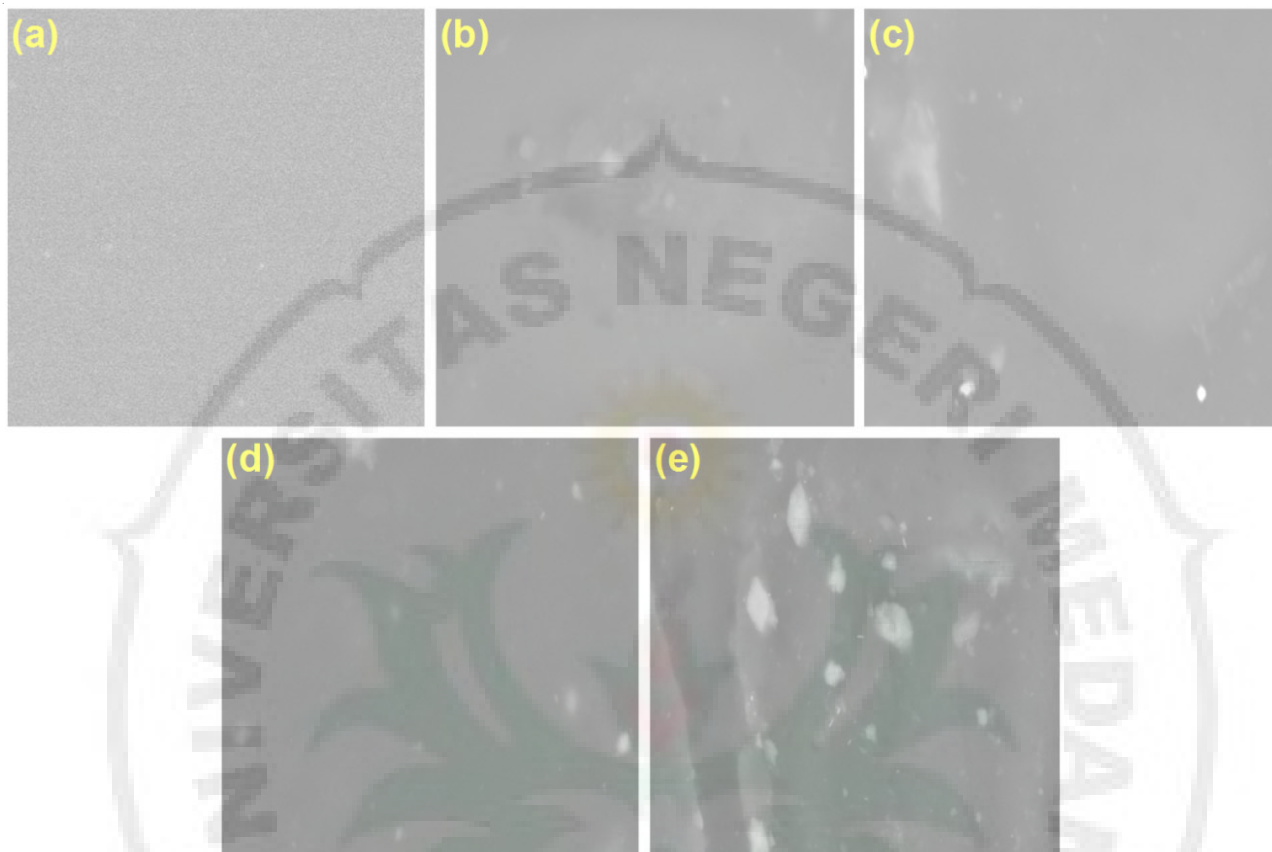


Fig. 5. SEM photograph of PVA/bentonite nanocomposites: (a) pristine PVA, (b) PVA/bentonite with 2 wt % bentonite, (c) PVA/bentonite with 4 wt % bentonite, (d) PVA/bentonite with 6 wt % bentonite, (e) PVA/bentonite with 8 wt % bentonite

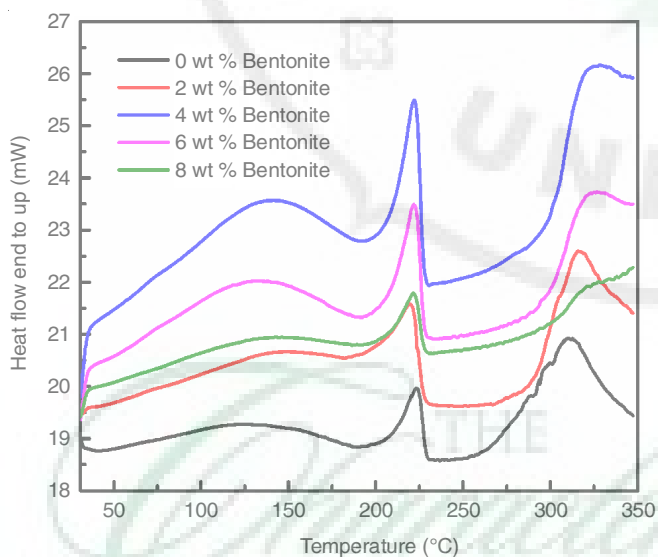


Fig. 6. Overlay thermogram of differential scanning calorimetry (DSC) from PVA/bentonite with bentonite varied 0-8 wt %

## Conclusion

Based on the results of mechanical tests of PVA/bentonite nanocomposites, the composition of bentonite (94:6) % gained an average value of the largest Young's modulus of 114.71 MPa. This mixture also obtained a uniform and homogenous morphology. Thermal properties is preferable to occur in the composition of 100:0 %, obtained the melting temperature of 223.51 °C with enthalpy of 27.10 J/g and the heat of 111.12 mJ.

## ACKNOWLEDGEMENTS

The authors acknowledge to Directorate of Research and Community Services, Directorate General of Higher Education that has funded this Prime Research Universities with the number contract of 045A/UN33.8/LL/2017. The authors also gratitude to the Rector and Chairman of Research Institute of Universitas Negeri Medan, Medan, Indonesia to support this research work.

## CONFLICT OF INTEREST

The authors declare that there is no conflict of interests regarding the publication of this article.

## REFERENCES

1. P.M. Ajayan, L.S. Schadler and P.V. Braun, *Nanocomposite Science and Technology*, WILEY-VCH Verlag GmbH Co. KGaA: Weinheim (2003).
2. P.H.C. Camargo, K.G. Satyanarayana and F. Wypych, *Mater. Res.*, **12**, 1 (2009); <https://doi.org/10.1590/S1516-14392009000100002>.
3. Y. Kojima, K. Fukumori, A. Usuki, A. Okada and T. Kurauchi, *J. Mater. Sci. Lett.*, **12**, 889 (1993); <https://doi.org/10.1007/BF00455608>.
4. S. Hashemian, H. Saffari and S. Ragabion, *Water Air Soil Pollut.*, **226**, 2212 (2015); <https://doi.org/10.1007/s11270-014-2212-6>.
5. R. Saboori, S. Sabbaghi, D. Mowla and A. Soltani, *Int. J. Nano Dimens.*, **3**, 101 (2012); <https://doi.org/10.7508/ijnd.2012.02.002>.
6. M. Sirait, N. Bukit and N. Siregar, *AIP Conf. Proc.*, **1801**, 020006 (2017); <https://doi.org/10.1063/1.4973084>.



7. M. George and T.E. Abraham, *J. Control. Rel.*, **114**, 1 (2006); <https://doi.org/10.1016/j.jconrel.2006.04.017>.
8. E. Frida, N. Bukit and M.H. Harahap, *J. Chem. Mater. Res.*, **3**, 10 (2013).
9. E.M. Ginting, N. Bukit, Muliani and E. Frida, *IOP Conf. Ser.: Mater. Sci. Eng.*, **223**, 012003 (2017); <https://doi.org/10.1088/1757-899X/223/1/012003>.
10. Y. Yang, C. Liu and H. Wu, *Polym. Test.*, **28**, 371 (2009); <https://doi.org/10.1016/j.polymertesting.2008.12.008>.
11. Y. Turhan, Z.G. Alp, M. Alkan and M. Dogan, *Micropor. Mesopor. Mater.*, **174**, 144 (2013); <https://doi.org/10.1016/j.micromeso.2013.03.002>.
12. M. Ferrández-Rives, Á. Beltrán-Osuna, J. Gómez-Tejedor and J. Gómez-Ribelles, *Materials*, **10**, 1448 (2017); <https://doi.org/10.3390/ma10121448>.
13. S. Sang, J. Zhang, Q. Wu and Y. Liao, *Electrochim. Acta*, **52**, 7315 (2007); <https://doi.org/10.1016/j.electacta.2007.06.004>.
14. H.S. Hassan, M.F. Elkady, A.H. El-Shazly and H.S. Bamufleh, *J. Nanomater.*, **2014**, 1 (2014); <https://doi.org/10.1155/2014/967492>.
15. P.B. Palani, R. Kannan, S. Rajashabala, S. Rajendran and G. Velraj, *Ionics*, **21**, 507 (2015); <https://doi.org/10.1007/s11581-014-1193-1>.
16. J.H. Chang, T.G. Jang, K.J. Ihn, W.K. Lee and G.S. Sur, *J. Appl. Polym. Sci.*, **90**, 3208 (2003); <https://doi.org/10.1002/app.12996>.
17. J.H. Chang, D.K. Park and K.J. Ihn, *J. Polym. Sci., B, Polym. Phys.*, **39**, 471 (2001); [https://doi.org/10.1002/1099-0488\(20010301\)39:5<471::AID-POLB1020>3.0.CO;2-6](https://doi.org/10.1002/1099-0488(20010301)39:5<471::AID-POLB1020>3.0.CO;2-6).
18. M. Yang, Y. Gao, J.P. He and H.M. Li, *Express Polym. Lett.*, **1**, 433 (2007); <https://doi.org/10.3144/expresspolymlett.2007.61>.
19. C. Zilg, R. Müllhaupt and J. Finter, *Macromol. Chem. Phys.*, **200**, 661 (1999); [https://doi.org/10.1002/\(SICI\)1521-3935\(19990301\)200:3<661::AID-MACP661>3.0.CO;2-4](https://doi.org/10.1002/(SICI)1521-3935(19990301)200:3<661::AID-MACP661>3.0.CO;2-4).
20. S.Y. Fu, X.Q. Feng, B. Lauke and Y.W. Mai, *Composites Part B*, **39**, 933 (2008); <https://doi.org/10.1016/j.compositesb.2008.01.002>.
21. T. Jose, S.C. George, M.M. G, H.J. Maria, R. Wilson and S. Thomas, *Ind. Eng. Chem. Res.*, **53**, 16820 (2014); <https://doi.org/10.1021/ie502632p>.
22. C. Johansson and F. Clegg, *J. Appl. Polym. Sci.*, **132**, 42229 (2015); <https://doi.org/10.1002/app.42229>.
23. A.A. Sapalidis, F.K. Katsaros, T.A. Steriotis and N.K. Kanellopoulos, *J. Appl. Polym. Sci.*, **123**, 1812 (2012); <https://doi.org/10.1002/app.34651>.
24. B.M. Kudaibergenova, M.K. Beisebekov, S.N. Zhumagalieva, M.M. Beisebekov, Z.A. Abilov and M.I. Chaudhary, *J. Chem. Soc. Pak.*, **35**, 1279 (2013).
25. T. Jose and S.C. George, *Polym. Plast. Technol. Eng.*, **55**, 1266 (2016); <https://doi.org/10.1080/03602559.2015.1132454>.
26. N. Bukit, S. Mekanik, Z. Tanpa and Z. Kalsinasi, *Makara Teknol.*, **16**, 121 (2012).

